APPLICATION OF ATMOSPHERIC CORRECTION TO HYPERSPECTRAL DATA: COMPARISONS OF DIFFERENT TECHNIQUES ON HYMAP DATA

Ian C Lau

Cooperative Research Centre for Landscape Environments and Mineral Exploration

The University of Adelaide, School of Earth and Environmental Science
Discipline of Geology and Geophysics, Adelaide, S.A. 5005

+61 (08) 8303 5493, +61 (08) 8303 4547
Ian.lau@adelaide.edu.au

Abstract

The interpretability of hyperspectral data is significantly influenced by the type and level of atmospheric correction performed. First pass corrections are often performed without in-depth consideration of scene specific features, which may result in a poorly corrected dataset. Noise and spurious absorptions due to poor correction hinder mineral identification and automated information extraction. Atmospheric correction involving the use of scene information and manual improvements produced superior results, although proved time consuming in comparison to radiative transfer software.

HyCorr, ACORN and empirical line techniques were used to correct the atmospheric features of a HyMap dataset from the Olary Domain, a semi-arid region of South Australia. The results were evaluated to determine the performance of various techniques with respect to the interpretability of spectral features.

Results from the HyCorr+EFFORT processing showed the average spectral response of the scene to display vegetation features and mineral absorptions. The visible and near-infrared regions displayed smooth spectral features, which corresponded well to areas that contained vegetation and iron oxides. The shortwave infrared region contained positive spikes and a kaolinitic spectral absorption for soils and outcrop. Shifting of the location of spectral absorptions in the shortwave infrared regions hampered identification of the features. Overall, this method produced deeper absorption features, with a compromise in the confidence of the spectral results.

HyCorr correction alone was found to produce a noisy spectral response with numerous positive spikes near water absorption bands and poor correction for some atmospheric gasses, such as CO_2. A limited trial was performed with ACORN to evaluate the software. The results found the insufficient correction for CO_2 gas in the ~2 µm region.

Samples were collected from the scene and measured in laboratory conditions for use in the empirical line calibration. An integrated method using HyCorr and empirical line correction was found to provide the best compromise with the least amount of noise and the most convincing spectral absorptions. This method required the most amount of computation as well as some *a priori* knowledge of the scene.

Introduction

The source of incident electromagnetic radiation (EMR) for passively acquiring remote sensors is the sun. The visible (VIS) (0.4-0.7 μm) near infrared (NIR) (0.7-1.3 μm) regions contain the maximum amount of solar energy, which falls off in energy into the shortwave infrared (SWIR) (1.3-2.5 μm). Electromagnetic radiation must travel through the atmosphere of Earth before interacting with surface materials.

Earth's atmosphere contains CO_2, O_2, O_3, H_2O, CH_4, CO, NH_4, N_2O, and other nitrogen gasses, which interact with Approximately 50% of the EMR spectrum over the region of 0.3-2.8 μm (Gao & Goetz, 1990a; Gao *et al.*, 1993). The gasses and particles in the atmosphere absorb and scatter significant amounts of the EMR over this region. The absorption features of these gases are typically narrow (figure 1), for example the O_2 features at 0.76 μm have individual width of 0.00 5 nm (Kurucz *et al.*, 1984). Particular regions of the EM spectrum, such as 0.9 μm, 1.1 μm, 1.4 μm and 1.9 μm wavelengths, are almost opaque to sensors. Regions that do not contain significant absorption features due to atmospheric gasses are called transmission windows (figure 2). It is these transmission widows that are exploited by remote sensing sensors.

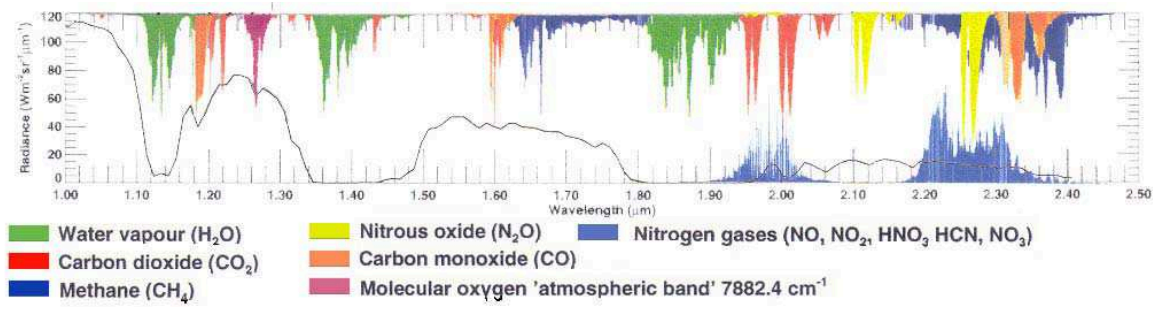

Figure 1 Absorption bands of atmospheric gases between 1.0 and 2.5 μm.

The CO_2, O_2, CH_4, CO and NH_4 gasses remain in relatively constant concentrations through the atmosphere, whereas O_3 predominantly occurs in the stratosphere. The concentration of H_2O can vary with altitude whereas the other gasses can differ with the environment setting. Aerosols over large cities have dissimilar concentrations than the rural atmosphere, which needs to be taken into account when using radiative models for correction.

Table 1 Atmospheric gasses and corresponding absorption features.

Gas	Absorption (μm)
H_20	0.94, 1.14, 1.38, 1.88 (Gao *et al.*, 1993) 0.69, 0.72, 0.76 (Aspinall *et al.*, 2002)
O_2	0.76, 0.6-1.3 (Gao *et al.*, 1993)
CO_2	2.01, 2.08 (Gao *et al.*, 1993) 1.6, 2.005, 2.055 (Aspinall *et al.*, 2002)
O_3	0.6 Chappius band (Gao *et al.*, 1993) 0.35, 9.6 (Aspinall *et al.*, 2002)
N_2O	2.0-2.5
CO	2.0-2.5
CH_4	2.35 (Gao *et al.*, 1993)

Atmospheric Correction

Atmospheric removal is performed to correct the spectral data for solar irradiance and atmospheric gas effects (Goetz *et al.*, 1985). Features relating to CO_2, which occur at 2.005 μm and 2.055 μm, are particularly important in the SWIR (Kneizys *et al.*, 1988). Data that has been poorly corrected for atmospheric effects can display absorption features at these wavelengths (figure 3b). Correction is required if the data is to be compared to a reference library (Clark, 1993; Kruse & Hauff, 1993) or laboratory spectral measurements.

Prior to atmospheric correction the raw DN data must first be corrected to remove sensor noise and scaled to correct for gains and offsets. There are a number of methods for removing atmospheric effects, which involve (1) the use of in data statistics, (2) modelling of the atmosphere from information within the data, (3) the use of ground based measurements from around the scene or (4) a combination of the above mentioned techniques.

Radiative Transfer (RT) Modelling

Radiative transfer models such as the ATmosphere REMoval (ATREM) program (Gao & Goetz, 1990b; Gao *et al.*, 1992; Gao *et al.*, 1993) use scene information and spectral features of the water vapour absorptions to model the theoretical atmosphere at the time of flight. This method attempts to correct for the solar irradiance atmospheric scattering and absorption as determined for the general conditions at the time of data acquisition. Each pixel is examined for water vapour by analysing the bands at 0.94 μm and 1.14 μm. Other gasses (O_2, O_3, CH_4, CO, CO_2 and N_2O), which absorb incident radiation causing noise in the data (table 1), are modelled using the inputted scene information. The

transmittance spectra of the atmospheric gasses are derived using the Malkmus narrow band model (Malkmus, 1967) based on the HITRAN 92 (Rothman *et al.*, 1992) database and the 5S (Simulation of the Satellite Signal in the Solar Spectrum) code (Tanré *et al.*, 1986), which is used to model scattering effects due to atmospheric molecules (Rayleigh scattering) and aerosols.

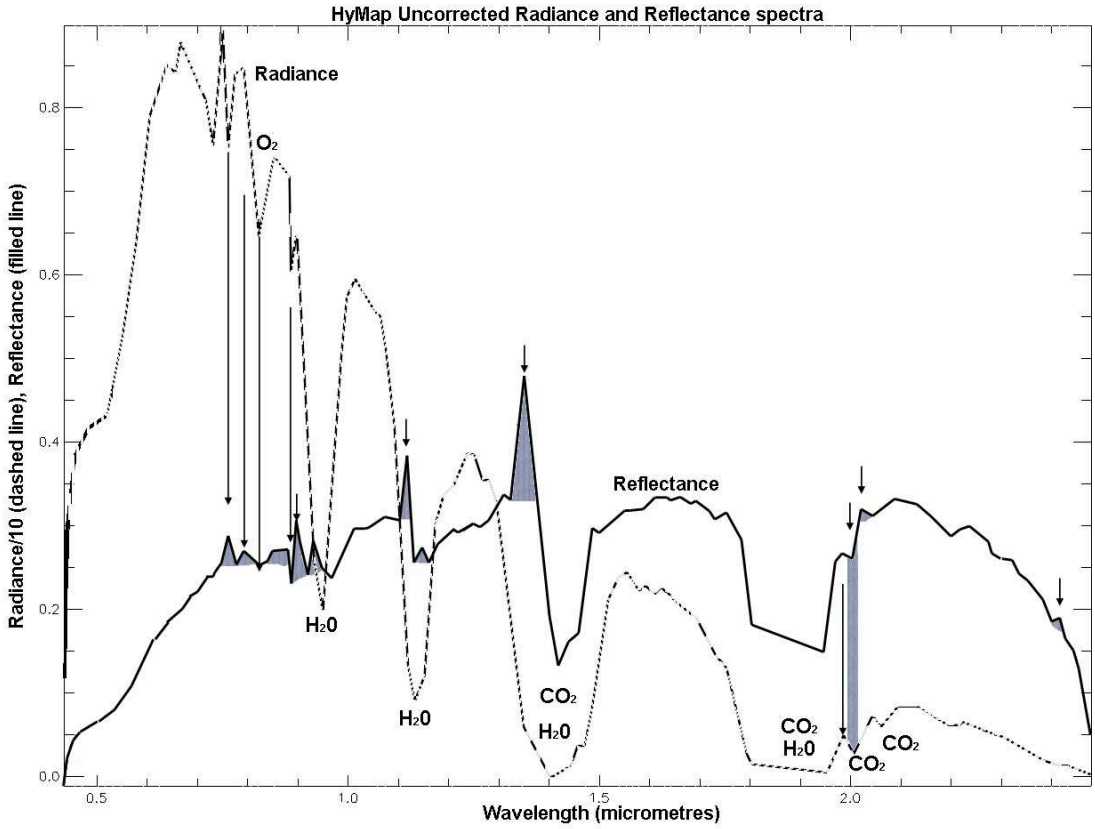

Figure 2 Hyperspectral Mapper (HyMap) uncorrected (radiance at sensor) and atmospherically corrected (reflectance) spectra from the Olary Domain. The characteristic shape of the uncorrected spectrum is due to the interactions of solar irradiated energy with the atmosphere. The shaded areas and arrows define poorly corrected regions of the reflectance spectrum. Distinguishable absorptions, due to gases in table 1, are shown.

User inputted information consisting of flight height, time, date, visibility and location (latitude and longitude) are used to calculate the solar zenith angle. The modelling uses the solar zenith angle to calculate information on the solar irradiance above the atmosphere, which can then be used to divide the radiance at sensor values to get apparent reflectance. Information on the dominant surface materials (green vegetation, iron oxides etc) are used to tweak the model. Relative depths of the water absorption bands are used to calculate the water vapour content of each pixel. This is used along with the transmittance spectra, derived from atmospheric gasses, to calculate scaled surface reflectance (Teliet, 1989; Gao & Goetz, 1990b; CSES, 1992). The advantage of RT techniques is the correction of hyperspectral data without *a priori* knowledge (Dwyer *et al.*, 1995).

There are a range of software programs available to model the atmosphere including ATREM (Gao & Goetz, 1990b; Gao *et al.*, 1992; CSES, 1999, ACORN (Atmospheric Correction Now) (Analytical Imaging and Geophysics LLC, 2002; Miller, 2002) HyCorr (Hyperspectral Correction), HATCH (High-Accuracy Atmosphere Correction for Hyperspectral Data) (Qu *et al.*, 2000; Goetz, 2002) and FLAASH (Fast Line-of-sight Atmospheric Analysis of Spectral Hypercubes) (Goetz, 2002). HyCorr was developed by CSIRO Division of Exploration and Mining Mineral Mapping Technologies Group (MMTG) based on ATREM and is the main software used in this research. Other RT models not mentioned above include MODTRAN (Berk *et al.*, 1998; Berk *et al.*, 1999) and LOWTRAN (Kneizys *et al.*, 1988), which operate in a similar manner to ATREM, but use additional ground based measurements to characterise the thermal structure and water content of the atmosphere (Aspinall *et al.*, 2002).

The ATREM software uses a three band ratioing technique in the region of the water absorption features to calculate the parameters of the atmospheric gases, which occur as high frequency features. This interpolation can induce errors in the radiative transfer model, resulting in the output scaled reflectance image possessing systematic errors and spikes (Berk *et al.*, 1989) (figure 2). The ATREM model does not account for the coupling effect between aerosol scattering and gaseous absorption, which predominantly occurs when viewing dark surfaces (Berk *et al.*, 1989). Problems also arise in the ATREM correction when the surface reflectance spectrum is not linear over the wavelengths where the three band ratioing technique is situated. Non-linear reflectance occurs in iron oxide rich soils and for wet green vegetation (Qu *et al.*, 2000). An attempt to counter this problem was integrated into the HyCorr software, which allows the option of using only the 1.14 µm region when the scene environment is rich in iron oxides.

Improvements to the Malkmus band model have been performed in HITRAN 96, 99 and 2000 (Rothman *et al.*, 2003), which were incorporated into newer atmospheric correction software such as HATCH and FLAASH. Unfortunately these programs were not available to the author at the time of this research to compare their performance.

Spectral smoothing

A spectral smoothing program called Empirical Flat Field Optimal Reflectance Transformation (EFFORT) (Boardman & Huntington, 1996; Boardman, 1998) can be used to remove the noisy features leftover after atmospheric correction. The EFFORT process examines the data to extract an average featureless spectrum by applying a Legendre polynomial fit to each spectra to determine how well it is modelled. A linear regression technique is used to calculate gains, which are applied to the featureless spectra to have the same appearance as the modelled spectra. These gains are applied to the remaining data to remove the noise and spikes. Spectral features of key minerals and other components (‘Reality Boosts”) in the scene can be applied to reinstate spectral features, which may have been removed as part of the noise.

Empirical Line (EL) Method

The use of spectral measurements of materials from within the scene using field or laboratory spectrometers to correct the airborne imagery has been well documented (Clark *et al.*, 2002). The term Empirical Line (EL) Calibration (Roberts *et al.*, 1985; Conel *et al.*, 1987; Kruse *et al.*, 1990) has been used for the technique where at least two materials with contrasting albedo (bright and dark) are used to correct spectral data. The technique requires a uniform area within the swath where field measurements are collected and deconvoluted to the imagery spatial bandwidths.

These averaged and deconvoluted field spectra are used to convert the data from at-sensor radiance values (microwatts per square centimetre per nanometre per steradian - $\mu W\ cm^{-2}\ nm^{-1}\ sr^{-1}$) to percent reflectance using a linear regression technique. A series of gains and offsets are calculated for each band based on the difference between the actual spectrum and the calculated spectrum, (Ben-Dor & Kruse, 1994; Dwyer *et al.*, 1995; Perry, 2000) The model assumes that the entire scene is topographically flat, with no scan angle or view angle effects (Perry, 2000), which causes problems when large variations in height occur in the data (Ferrier, 1995). Complications may occur with locating the sample pixel on the ground or conversely, the field site where the sample was collected in the imagery.

The HyMap Sensor and Area of Research

HyMap (Hyperspectral Mapper) was developed through a joint effort of Integrated Spectronics and the Optical Systems Engineering group of the CSIRO Manufacturing Science and Technology. The instrument is an airborne hyperspectral scanner with the versatility of operating from a light aircraft with a standard camera port. HyMap has a high signal to noise ratio (>500:1) and a high spatial resolution (2-10 m depending on flight height), with spectral coverage in VIS, NIR and SWIR. The scanner provides 128 wavelength channels with bandwidths generally in 10 - 20 nm range. The high SNR and spatial resolution allows greater discrimination between noise and sub-pixel features. A detailed explanation of the calibration of the instrument can be found in Cocks *et al*. (1998).

The HyMap data used in this analysis consisted of 5 runs acquired in November 1998. The data has a spectral resolution of 5m and an average overlap of 500m between the sub-parallel swaths. The coverage area consists of a regolith-dominated terrain of highly-weathered saprolite of the Palaeoproterozoic Willyama Supergroup, Mesoproterozoic granitoids and Adelaidean metasediments, which are variably covered by a alluvial and colluvial sediments. The region hosts a number of significant sites of Cu-Au mineralisation, including the White Dam Prospect (McGeough & Anderson, 1998; Cooke, 2003).

Atmospheric correction

The Raw HyMap data were received from MIM Exploration and Mining in an unprocessed state. Each raw swath consisted of two portions, which were

required to be mosaiced into full lines before any further processing was performed. A calibration file was obtained from HyVista and the data were atmospherically corrected using HyCorr at PIRSA by Dr. Alan Mauger. EFFORT polishing was also applied as a subroutine of. During the preliminary correction a full suite of 'Reality Boosts' were used in the EFFORT processing. HyCorr was found to overestimate the abundance of water vapour, causing problems in the 0.94-1.130 µm and 1.380-1.870 µm regions (figure 2). The 0.76 µm O_2 and 2.005 µm and 2.055 µm CO_2 absorption features were also found to be problematic, resulting in negative spikes around these wavelengths (Kneizys *et al.*, 1988; Staenz *et al.*, 2002).

The boosted EFFORT algorithm was found to introduce green vegetation and kaolinite features into the spectra of each pixel of the data. The absorption features were found to be more difficult to resolve and identification of the constituent materials were hindered by the persistent presence of the 2.16 µm absorption, red edge feature at 0.76 µm and a reflectance peak at 2.33 µm. Absorption features in the 2.25-2.4 µm region were denuded or replaced by two sharp absorptions at 2.304 µm and 2.401 µm (figure 3a) due to the induced reflectance high at 2.33 µm. The positions of the Al-OH absorption features in the 2.16-2.2 µm region were found to be broadened or shifted to different wavelengths by the EFFORT and reality boost processes.

A detailed analysis was carried out on the different settings of the HyCorr software, involving the trialling of a diverse combination of the programs parameters. The use of EFFORT without any Reality Boost parameters resulted in a featureless spectrum devoid of identifiable absorptions in the SWIR region (figure 3f). The data were found to be almost unusable for processing as most of the absorption features were not resolvable or identifiable, however the VNIR produced highly comparable results for Fe-rich soils and other ferruginous materials (figure 3f).

HyCorr corrected data, without EFFORT polishing (figure 3b), were found to contain numerous high amplitude positive and negative spikes that were inferred to be errors in the radiative transfer model. The larger features appeared to be additive and were reduced by the use offset coefficients (figure 3e), which were calculated using the average spectrum of the swath. The average spectral response and the standard deviation were normalised resulting in a value for each band. The generated values were added back to the spectra of each pixel within the swath using ENVI. This method produced a 'cleaner' spectrum that appeared to correspond better to reference spectra (USGS Digital Spectral Library (Clark, 1993) and field spectrometer measurements (figure 3e), although a number of unwanted absorption features persisted in the spectra.

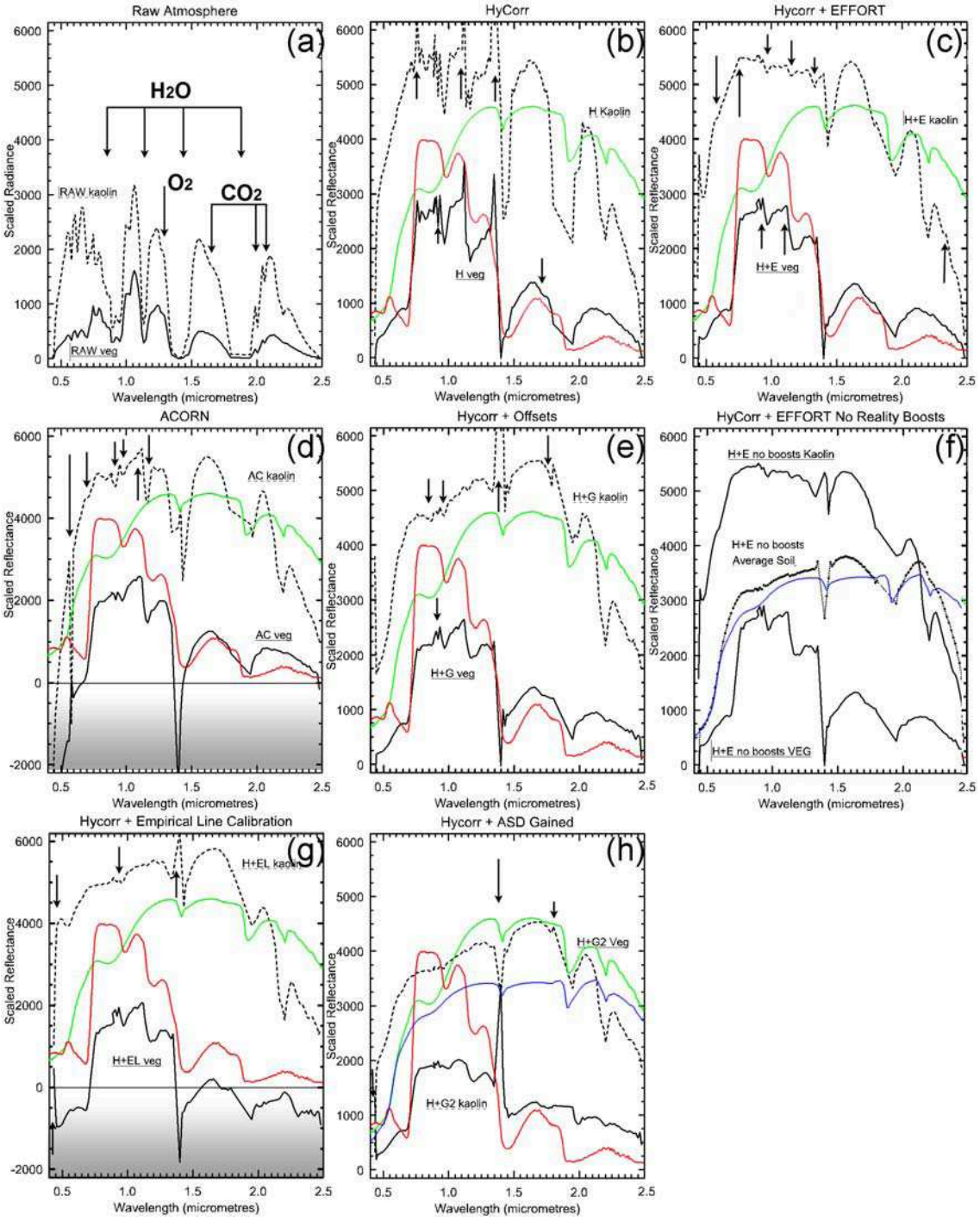

Figure 3 Comparison of various atmospheric correction results with the raw data (a). ASD FieldSpec measurements for the corresponding pixels containing the eucalyptus vegetation, kaolinite saprolite and an average soil spectrum are shown in red, green and blue respectively. The results from the ACORN (d) and Empirical Line calibration corrections (g) are scaled to account for their negative values.

From the observation of the difference between the ASD FieldSpec measurements of field samples and the airborne data processed by the above methods, it was concluded that an empirical line (EL) approach would produce the most comparable spectra to field and reference data. A quarry excavated

for road materials was used as a bright target and the road was used as the dark target. Samples were collected from the locations in November 2001, November 2002 and March 2003 and measured using an ASD FieldSpec FR in April 2003. A small piece of bitumen was chipped off of the edge of the road for the dark target and light-coloured rounded carbonate/weathered saprolite lag material was collected from a homogeneous region in the quarry. The ASD measurements were resampled to HyMap wavelengths and the empirical line calibration performed within ENVI version 3.5.

The resulting EL calibration for the HyMap swath contained mixed results. The laboratory spectra collected with the ASD FieldSpec were found to be comparable to the EL calibrated HyMap data and were especially coherent in the NIR and SWIR regions (figure 3f). The data were found to contain negative values in the shorter wavelengths, which was attributed to poorly chosen regions of interest for the dark pixels within the imagery or the asphalt sample not representing the bitumen road of the HyMap imagery. On examination of the field area, the bitumen road was found to be less than an ideal dark target as the worn asphalt in the centre of the road appeared a shade of light grey. This contrasted the dark, freshly tarred edges, where the samples were collected. Without a sufficient dark target for correction, a modified empirical method was required to be implemented.

The modified empirical line technique used sampled sites where ASD measurements had been collected to further improve the calibration of the HyCorr corrected data, in a similar manner as the offset method. Average HyMap spectra for the sample sites were collected and used to calculate gains by dividing with the corresponding ASD FieldSpec measurements. These gains were applied back to each pixel using the Band Math function in ENVI. The results produced spectra with a clean, smooth appearance and a greater variability in shape of the hull (figure 3h), unlike the HyCorr corrected data (figure 3b, c, e, f & g). The spectra from empirical line corrected data were found to be comparable to ASD FieldSpec measurements of samples from within the swath. (figure 4).

The ASD FieldSpec (>2000 bands) measurements of samples collected from within the swath area were resampled to the HyMap wavelengths (128 bands). The ASD spectra were then used with the spectrum of the corresponding pixel from the imagery to normalise the HyMap data. The normalisation process involved dividing the HyMap data by 10000 to reduce it to % reflectance values, to match the units of the ASD FieldSpec measurements, and dividing the results by the re-sampled ASD FieldSpec measurements. The normalised data were then compared to the other regions to determine which were the flattest and had values closest to zero. The normalised spectra with the closest match to the reference library were chosen for the calculation of the gains.

The calibration gains were used to correct the four remaining swaths. The spectra of the overlap regions of the swaths were examined for consistency (figure 4). Differences between the swaths were found to be minimal, with minor variation in the reflectance levels between the swaths. Absorption

features between swaths had similar wavelengths for all the regions examined (figure 4). A strong similarity was found with ASD measurements of collected samples from the corresponding locations (figure4b).

The technique described above is similar to the Reflectance-Mean Normalisation (RMN) technique, used by Bierwirth (2000, 2002), where smoothing process of the EFFORT correction was found to denude or completely removing diagnostic mineral absorption features and as a consequence decreased the efficiency of the mineral mapping techniques. The technique was applied to address the problems encountered when comparing reference and field derived spectra with the ATREM-EFFORT corrected HyMap data.

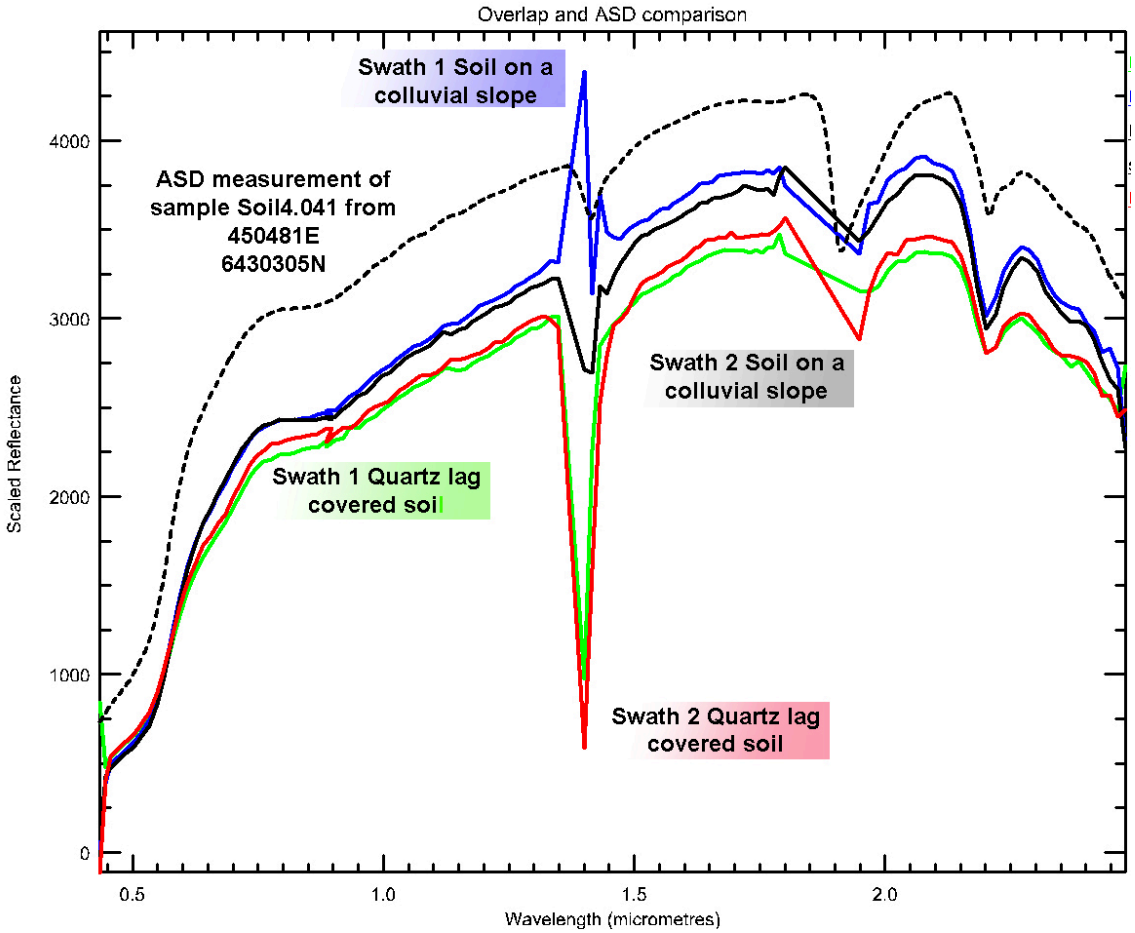

Figure 4 Comparison of co–registered pixels from adjacent HyMap swaths corrected by the HyCorr+ ASD Gains method (figure 3g). The dashed spectrum is a ASD FieldSpec measurement of samples collected from the corresponding pixel area.

A second radiative transfer atmospheric correction program was briefly trialled as a comparison to the HyCorr software. The results from the ACORN program found the SWIR region was highly comparable to the HyCorr + EFFORT result, although the left shoulder of the kaolinite feature was shifted to shorter wavelengths, causing the feature to broaden. The ACORN correction displayed a small absorption feature at 2.0 µm, related to CO_2 gas. Bright materials were found to have negative values for the near UV region (<0.5 µm),

with dark materials an even greater region (<0.7μm). An unexpected deep absorption feature at 0.6 μm, a shoulder feature at 0.7μm and high frequency, low amplitude absorptions in the NIR showed that the correction software also displayed difficulties in correcting for atmospheric effects. It is the authors view that these errors can be removed with careful use of input parameters in the radiative transfer software and the application of correctional offsets during post-atmospheric processing.

A point not considered by this paper is the effect of topography on the correction of remotely sensed data. Topography can influence the spatial and spectral characteristics of a dataset, especially in extremely rugged terrain.

Conclusions

Analysis of hyperspectral imagery for phyllo-silicate minerals and alteration products would require a technique with the greatest accuracy in the >2.0 μm region, therefore an empirical line correction is the ideal calibration technique. The EL calibration technique can improve the results for the VNIR region. If the location of the imagery was in an inaccessible area, the model based technique should be able to produce sufficient results to produce identifiable spectra, although the calculation of offsets to correct for the inefficiencies of the radiative transfer model would be required to visually improve the spectra. Care should be taken before applying an atmospheric correction program with consideration of the effects that the input parameters will have on the outcome.

Acknowledgements

Thank you to CRC LEME for funding of this research and for the use of the ASD. Data was supplied by MIMEX Pty Ltd and software by CSIRO Division of Exploration and Mining, Mineral Mapping Technologies Group. Thanks goes to Tom Cudahy and Rob Hewson for their technical help throughout the research period. The author wished to acknowledge Graham Heinson, Alan Mauger and Patrick James for their supervisory duties over the duration of the PhD.

References

ANALYTICAL IMAGING AND GEOPHYSICS LLC, 2002, ACORN 4.0 User's Guide: ImSpec LLC).

ASPINALL, R. J., MARCUS, W. A., and BOARDMAN, J. W., 2002, Considerations in collecting, processing, and analysing high spatial resolution hyperspectral data for environmental investigations. journal of Geographical Systems, 4, 15-29.

BEN-DOR, E., and KRUSE, F. A., 1994, The relationship between the size of spatial subsets of GER 63 channel scanner data and the quality of the internal average relative reflectance (IARR) atmospheric correction technique. International Journal of Remote Sensing, 15, 683-690.

BERK, A., ANDERSON, G. P., BERNSTEIN, L. S., ACHARYA, P. K., DOTHE, H., MATHEW, M. W., ALDER-GOLDEM, S. M., CHETWYND, J. H., RICHTSMEISER, S. C., PAKALL, B., L, A. C., JEONG, J. S., and HOKE, M. L., 1999, MODTRAN 4 Radiative Transfer Modelling for Atmospheric Correction. Summaries of the 8th Annual JPL Airborne Earth Science Workshop, Jet Propulsion Laboratory Publication Vol 1. AVIRIS Workshop, Jet Propulsion Laboratory, California Institute of Technology, Pasadena, California.

BERK, A., BERNSTEIN, L. S., ANDERSON, G. P., ACHARYA, P. K., ROBERTSON, D. C., CHETWYND, J. H., and ALDER-GOLDEM, S. M., 1998, MODTRAN cloud and multiple scattering upgrades with application to AVIRIS. Remote Sensing of Environment, 65, 367-375.

BERK, A., BERNSTEIN, L. S., and ROBERTSON, D. C., 1989, MODTRAN: a moderate resolution model for LOWTRAN7. In GL-TR-89-0122 (Hanscom Air Force Base, MA: Air Force Geophysics Laboratories), pp. 28.

BIERWIRTH, P., HUSTON, D., and BLEWETT, R. S., 2002, Hyperspectral mapping of mineral assemblages associated with gold mineralization in the central Pilbara, Western Australia. In A special issue devoted to the early to middle Archean mineral deposits of the North Pilbara Terrain, Western Australia., edited by L. Houston David, H. Hickman Arthur, and L. F. Collins Peter: Economic Geology Publishing Company. Lancaster, PA, United States. 2002.).

BIERWIRTH, P. N., 2000, Hyperspectral mineral mapping and gold prospecting in a low bedrock exposure terrain using HyMap in the West Pilbura, W.A., Australia. Proceedings of the 10th Australasian Remote Sensing Conference, Adelaide, 814-825.

BOARDMAN, J. W., 1998, Post-ATREM polishing of AVIRIS apparent reflectance data using EFFORT: a lesson in accuracy versus precision. Summaries of the 7th JPL Airborne Earth Science Workshop, JPL Publication 97-21, 53.

BOARDMAN, J. W., and HUNTINGTON, J. F., 1996, Mineral Mapping with 1995 AVIRIS Data. Summaries of the 6th Annual JPL Airborne Earth Science Workshop, Jet Propulsion Laboratory Publication 96-4 Vol 1. AVIRIS Workshop, Jet Propulsion Laboratory, California Institute of Technology, Pasadena, California.

CLARK, R. N., 1993, The USGS Digital Spectral Library. In USGS Open file report (Reston, Virginia, pp. 93-592.

CLARK, R. N., SWAYZE, G. A., LIVO, K. E., KOKALY, R. F., KING, T. V. V., DALTON, J. B., VANCE, J. S., ROCKWELL, B. W., HOEFEN, T., and MCDOUGAL, R. R., 2002, Surface Reflectance Calibration of Terrestrial Imaging Spectroscopy Data: a Tutorial Using AVIRIS, U. S. Geological Survey.

COCKS, T., JENSSEN, R., STEWARD, A., WILSON, I., and SHIELDS, T., 1998, The HyMapTM airborne hyperspectal sensor: The system, calibration and performance: Proceedings 1st EARSeL workshop on Imaging Spectroscopy, 6-8 October 1998, p. 37-43.

CONEL, J. E., GREEN, R. O., VANE, G., BRUEGGE, C. J., and ALLEY, R. E., 1987, Airborne Imaging Spectrometer-2: Radiometry and a comparison of methods for the recovery of ground reflectance. Proceedings, Airborne Imaging Spectrometer Data Analysis Workshop, Jet Propulsion Laboratory 87-30, Pasadena, California, 18-47.

COOKE, A., 2003, White Dam- an exciting new gold project in the Curnamona Province. MESA Journal, 31, 4-5.

CSES, 1999, ATmosphere REMoval Program (ATREM) User's Guide Version 3.1, Center for the Study of Earth from Space (Boulder, Colorado: University of Colorado).

CSES, C. F. T. S. O. E. F. S., 1992, ATmosphere REMoval Program (ATREM) Version 1.1 July 1997 (Boulder, Colorado: University of Colorado).

DWYER, J. L., KRUSE, F. A., and LEFKOFF, A. B., 1995, Effects of empirical versus model-based reflectance calibration on automated analysis of imaging spectrometer data; a case study from the Drum Mountains, Utah. Photogrammetric Engineering and Remote Sensing, 61, 1247-1254.

FERRIER, G., 1995, Evaluation of apparent surface reflectance estimation methodologies. International Journal of Remote Sensing, 16, 2291-2297.

GAO, B., and GOETZ, A. F. H., 1990a, Column atmospheric water vapor and vegetation liquid water retrievals from airborne imaging spectrometer data. Journal of Geophysical Research, 95(D-4), 3549-3564.

GAO, B., and GOETZ, F. H., 1990b, Column atmospheric water vapor and vegetation liquid water retrievals from airborne imaging spectrometer data. Journal of Geophysical Research, 95, 3549-3564.

GAO, B. C., HEIDEBRECHT, K., and GOETZ, A. F. H., 1992, Software for the derivation of scaled surface reflectances from AVIRIS Data. Summaries of the Third annual JPL airborne geoscience workshop; Volume 1 AVIRIS workshop.

GAO, B. C., HEIDEBRECHT, K. B., and GOETZ, A. F. H., 1993, Derivation of scaled surface reflectances from AVIRIS data. Remote Sensing of Environment, 44, 165-178.

GOETZ, A., 2002, Relative performance of HATCH and three other techniques for atmospheric correction of Hyperion and AVIRIS data: EO-1 Science Validation Meeting.

GOETZ, A. F. H., VANE, G., SOLOMON, J. E., and ROCK, B. N., 1985, Imaging spectrometry for earth remote sensing. Science, 228, 1147-1153.

KNEIZYS, F. X., SHETTLE, E. P., ABREAU, L. W., CHETWYND, J. H., ANDERSON, G. P., GALLERY, W. O., SELBY, E. A., and CLOUGH, S. A., 1988, Users guide to LOWTRAN-7. In AFGL-TR-8-0177 Air Force Geophysics Laboratories (Bedford, Massachusetts, pp. 137.

KRUSE, F. A., and HAUFF, P. L., 1993, The IGCP=264 Spectral Properties Database. In AGU Special Publication (Washington, DC: American Geophysical Union), pp. 211.

KRUSE, F. A., KIEREIN-YOUNG, K. S., and BOARDMAN, J. W., 1990, Mineral mapping at Cuperite, Nevada, with a 63 channel imaging spectrometer. Photogrammetric Engineering & Remote Sensing, 56, 83-92.

KURUCZ, R. L., FURENLID, I., BRAULT, J., and TAESTERMAN, L., 1984, Solar Flux Atlas from 296 to 1300nm. In National Solar Observatory Atlas No.1 (Sunspot, NM: National Solar Observatory), pp. 163-165.

MALKMUS, W., 1967, Random Lorentz band model with exponetial tailed S line intensity distribution function. Journal of the Optical Society of America, 57, 323-329.

MCGEOUGH, M., and ANDERSON, J., 1998, Discovery of the White Dam Au-Cu mineralisation: Broken Hill Exploration Initiative: Abstracts of papers presented at forth annual meeting.

MILLER, C. J., 2002, Performance assessment of ACORN atmospheric correction algorithm: Algorithms and Technologies for Multispectral, Hyperspectral, and Ultraspectral Imagery VIII; Aerosense 2002.

PERRY, E. M., WARNER, T., FOOTE, P., 2000, Comparison of atmospheric modelling versus empirical line fitting for mosaicking HYDICE imagery. International Journal of Remote Sensing, 21, 799-803.

QU, Z., GOETZ, A. F. H., and HEIDEBRECHT, K. B., 2000, High-Accuracy Atmosphere Correction for Hyperspectral Data (HATCH). Summaries of the 9th Annual JPL Airborne Earth Science Workshop, Jet Propulsion Laboratory Publication Vol 1. AVIRIS Workshop, Jet Propulsion Laboratory, California Institute of Technology, Pasadena, California.

ROBERTS, D. A., YAMAGUCHI, Y., and LYON, R. J. P., 1985, Calibration of airborne imaging spectrometer data to percent reflectance using field spectral measurements. Proceedings, Nineteenth International Symposium on Remote Sensing of Environment, Ann Arbor, Michigan, 21-25 October, 679-688.

ROTHMAN, I. S., GAMACHE, R. R., and C, C. A., 1992, The HITRAN molecular database: editions of 1991 and 1992. Journal of Quantitative Spectroscopy & Radiative Transfer, 48, 469-507.

ROTHMAN, L. S., BARBE, A., BENNER, D. C., BROWN, L. R., CAMY-PEYRET, C., CARLEER, M. R., CHANCE, K., CLERBAUX, C., DANA, V., DEVI, V. M., FAYT, A., FLAUD, J. M., GAMACHE, R. R., GOLDMAN, A., JACQUEMART, D., JUCKS, K. W., LAFFERTY, W. J., MANDIN, J. Y., MASSIE, S. T., NEMTCHINOV, V., NEWNHAM, D. A., PERRIN, A.,

RINSLAND, C. P., SCHROEDER, J., SMITH, K. M., SMITH, M. A. H., TANG, K., TOTH, R. A., VANDER AUWERA, J., VARANASI, P., and YOSHINO, K., 2003, The HITRAN molecular spectroscopic database: edition of 2000 including updates through 2001. Journal of Quantitative Spectroscopy & Radiative Transfer, 82, 5-44.

STAENZ, K., SECKER, J., GAO, B. C., DAVIS, C., and NADEAU, C., 2002, Radiative transfer codes applied to hyperspectral data for the retrieval of surface reflectance. ISPRS Journal of Photogrammetry & Remote Sensing, 57, 194-203.

TANRÉ, D., DEROO, C., DUHAUT, P., HERMAN, M., MORCHRETTE, J. J., PERBOS, J., and DESCHAMPS, P. Y., 1986, Simulation of the Saellite Signal in the Solar Spectrum (5S) Users Guide, Laboratoire d'Optique Atmospherique, U.S.T. de Lille, 59655 Villeneuve d'ascq, France.

TELIET, P. M., 1989, Surface reflectance retrieval using atmospheric correction algorithms. Proceedings, of IGARSS'89 and the 12th Canadian Symposium on Remote Sensing, Vancouver, Canada, 864-867.